

Article

Electrochemical Properties of NiCo₂O₄/WO₃/Activated Carbon Wheat Husk Nano-Electrocatalyst for Methanol and Ethanol Oxidation

Mohammad Bagher Askari ^{1,*}, Parisa Salarizadeh ², Seyed Rouhollah Samareh Hashemi ³, Mohsen Shojaeifar ⁴  and Sadegh Azizi ⁵

¹ Department of Semiconductor, Institute of Science and High Technology and Environmental Sciences, Graduate University of Advanced Technology, Kerman P.O. Box 7631818356, Iran

² High-Temperature Fuel Cell Research Department, Vali-e-Asr University of Rafsanjan, Rafsanjan P.O. Box 7718897111, Iran; p.salarizadeh@vru.ac.ir

³ Department of Fiber Optics, Institute of Science and High Technology and Environmental Sciences, Graduate University of Advanced Technology, Kerman P.O. Box 7631818356, Iran; s.r.hashemi@gmail.com

⁴ Department of Laser, Institute of Science and High Technology and Environmental Sciences, Graduate University of Advanced Technology, Kerman P.O. Box 7631818356, Iran; m.shojaeifar@kgut.ac.ir

⁵ Department of Physics, Faculty of Science, University of Guilan, Rasht P.O. Box 41335-1914, Iran; sazizi@msc.guilan.ac.ir

* Correspondence: mbaskari@phd.guilan.ac.ir

Abstract: It is common to use efficient catalysts in the anodes and cathodes of methanol and ethanol fuel cells, such as platinum and ruthenium. However, due to their expansivity and rarity, finding a suitable alternative is important. In this work, multi-component catalysts consisting of tungsten oxide, nickel cobaltite, and activated carbon were synthesized through the hydrothermal method. The performance of catalysts in the processes of methanol and ethanol oxidation reactions (MOR and EOR) were investigated. The addition of activated carbon obtained from wheat husk, with an excellent active surface and acceptable electrical conductivity, to the matrix of the catalyst significantly facilitated the oxidation process of alcohols and enhanced the efficiency of the catalyst. The physical and electrochemical characterization of the NiCo₂O₄/WO₃ hybridized with the wheat husk-derived activated carbon (ACWH) catalyst indicated its successful synthesis and good performance in the alcohol oxidation process. NiCo₂O₄/WO₃/ACWH with an oxidation current density of 63.39 mA/cm² at the peak potential of 0.58 V (1.59 vs. RHE), a cyclic stability of 98.6% in the methanol oxidation reaction (MOR) and 27.98 mA/cm² at the peak potential of 0.67 V (1.68 vs. RHE), and a cyclic stability of 95.7% in the ethanol oxidation reaction (EOR) process can be an interesting option for application in the anodes of alcohol fuel cells.

Keywords: NiCo₂O₄/WO₃; activated carbon wheat husk; MOR; EOR; alcohol fuel cells



Citation: Askari, M.B.; Salarizadeh, P.; Samareh Hashemi, S.R.; Shojaeifar, M.; Azizi, S. Electrochemical Properties of NiCo₂O₄/WO₃/Activated Carbon Wheat Husk Nano-Electrocatalyst for Methanol and Ethanol Oxidation. *Catalysts* **2024**, *14*, 302. <https://doi.org/10.3390/catal14050302>

Academic Editor: Nicolas Alonso-Vante

Received: 25 January 2024

Revised: 26 April 2024

Accepted: 29 April 2024

Published: 2 May 2024



Copyright: © 2024 by the authors. Licensee MDPI, Basel, Switzerland. This article is an open access article distributed under the terms and conditions of the Creative Commons Attribution (CC BY) license (<https://creativecommons.org/licenses/by/4.0/>).

1. Introduction

One of the most important goals of sustainable development is providing clean energy at a suitable and affordable price [1]. Therefore, investing in the field of energy production from renewable fuel sources such as solar, wind, and thermal energy, along with improving energy efficiency from current fossil fuel sources, is vital to guarantee energy production for the coming years [2]. Expanding infrastructure and upgrading technology to provide energy from clean fuel sources in all countries will encourage economic growth and help the environment [3]. Although the energy crisis and the limitation of the use of fossil fuels for electricity production is a serious issue in a world that is highly dependent on energy, electricity is still produced from fossil fuels in most parts of the world [4]. Sustainable development is impossible without having a pattern of energy consumption and detailed planning of countries to replace new fuel sources [5].

In addition to renewable fuel sources, clean fuels can solve the energy crisis [6]. Biofuel, methanol, ethanol, etc., are considered to be clean fuels [7]. Considering the predictable lack of energy sources in the future, the direct consumption of methanol and ethanol as clean fuels for fuel cell devices will be of great interest [8].

In fuel cells, compounds such as methanol, ethanol, propanol, ethylene glycol, etc., can be used as fuel [9]. Fuel cells have advantages such as easy access to fuel, low polluting production, and high efficiency [10]. The importance of using portable equipment with relatively good performance has drawn much attention to fuel cells in recent years [11].

The lack of energy and fossil fuel resources and the destructive effects that the excessive use of these fuels have on environmental conditions and human health have provided mankind with a big and costly challenge [12]. Undoubtedly, one of the important factors in achieving economic stability and developing environmental sustainability is paying attention to the issue of energy and the excessive consumption of fossil fuel resources [13]. In the short-term and long-term development plans of most countries, special attention has been paid to energy production, storage, and supply, so it can be said that an energy-based economy is an essential issue in the developing world [14].

With the progress made in nanoscience and interdisciplinary scientific activities in recent years, we have witnessed the emergence of ultra-modern equipment in the field of energy storage and production with excellent efficiency [15]. Batteries and supercapacitors are used for energy storage [16], and fuel cells for energy production [17].

There are different types of fuel cells. Direct alcohol fuel cells, due to some advantages such as the availability and abundance of alcohol fuel, their relatively low operating temperature, and their simple structure [18,19], have received more attention than others. The structure of these fuel cells includes an anode, a cathode, and a separating membrane [20]. Fuel (methanol, ethanol, etc.) electro-oxidation and oxygen reduction take place in the anode and cathode, respectively [21].

The most efficient catalysts for fuel cells are generally based on platinum and ruthenium [22]. However, there are some limitations, such as rarity, high cost, and unavailability. Today, one of the most attractive fields of interdisciplinary science is designing, manufacturing, and proposing new catalysts to replace expensive catalysts in the structure of fuel cells. The introduction of stable and high-efficiency electrode materials in the field of energy production and storage has been noticed by researchers.

Cobalt, nickel, cerium, and manganese elements in the forms of oxide and sulfide have shown excellent ability to oxidize alcohols [23–25]. In addition to these materials, binary transition metal oxides [26] and binary transition metal sulfides are of great interest as catalysts for fuel cells. It should be mentioned that the combination of metal sulfides/oxides in binary or ternary forms causes a synergistic effect between metal ions and thus improves the electrocatalytic behavior of the catalyst. NiCo_2O_4 [27], MnCo_2O_4 [28], CoFe_2O_4 [29], and NiFe_2O_4 [30] are among these catalysts that are widely investigated as fuel cell anodes and cathode electrodes. It should be noted that the most theoretically proven use of these materials is in the electrodes of supercapacitors for energy storage [31]. Placing metal oxides and especially transition metal oxides next to each other creates a significant synergistic effect in electrochemical processes. For example, mixing metal oxides such as Co_3O_4 , Fe_3O_4 , CeO_2 , MnO_2 , ZnO , and NiO creates good intrinsic electrocatalytic activity. For example, research in which the catalysts $\text{Co}_3\text{O}_4/\text{NiO}$ [32], $\text{NiO-MOF}/\text{rGO}$ [33], NiO/Ni [34], FeO/NiO MOF [33], $\text{CeO}_2\text{-NiO-rGO}$ [35], and $\text{Mn}_2\text{O}_3@ \delta\text{-MnO}_2$ [36] were evaluated in the oxidation process of alcohols bears mentioning. Additionally, NiCo_2O_4 nanoparticle-anchored graphene microspheres and $\text{NiCo}_2\text{O}_4/\text{reduced graphene oxide}$ were reported as electrodes of supercapacitors [37,38]. These materials showed high specific capacitance and excellent cycling stability. NiCo_2O_4 shows better electrochemical activity than individual oxides (NiO and Co_3O_4) due to higher electronic conductivity. In addition, it is low-cost, easily available, and has excellent corrosion stability in alkaline media [39,40].

Metal oxides suffer from low electrical conductivity and relatively low active surface area. To solve these defects, strategies such as doping of elements to their structures, adding

carbon materials to the matrixes of metal oxides, and adding of polymeric materials have been used.

Among the additives that are added to the structures of catalysts to improve their conductivity and electrochemically active surface, carbon is a suitable option due to its abundance in nature. In addition to carbon materials, zeolites, MXenes, and metal–organic frameworks (MOFs) can be helpful. By increasing the active surface area, they also improve the electrocatalytic activity. Among all the mentioned substrates, carbon materials, with their extraordinary physical and chemical properties, increase the active surface and improve the catalyst's electrical conductivity [41]. High active surface area and good electrical conductivity are important factors for a catalyst to be considered efficient. Among the conventional carbon structures, single-walled and multi-walled carbon nanotubes, activated carbon, graphene, and carbon quantum dots can be mentioned. Activated carbon has attracted the attention of our research team due to its wide variety.

Tungsten trioxide (WO_3) is a promising n-type semiconductor oxide with a band gap of 2.6–2.8 eV for photocatalytic reactions [42]. Additionally, it possesses non-toxicity and cost-effectiveness. Therefore, it has high potential in electrocatalyst, electrochemical energy storage and in photoelectrochemical water splitting applications. The application of this metal oxide in the form of a multi-component composite in energy production and energy storage and in the detection of very small amounts of various drugs has been studied a lot [43–45]. NiCo_2O_4 is one of the most famous and widely used binary metal oxides. The synergistic effect of hybridizing and placing nickel and cobalt metal oxides next to each other has introduced this material as a highly efficient catalyst in various fields of electrochemistry. The use of this material in the anodes and cathodes of fuel cells [46], the electrodes of batteries [47] and supercapacitors [48], and as a highly active catalyst in the field of detection has been studied [49]. In this research, activated carbon with a very high active surface was synthesized from wheat husk, and by adding it to the structure of metal oxides NiCo_2O_4 and WO_3 , the efficiency of the proposed catalysts in the process of methanol and ethanol oxidation was evaluated.

In the present study, WO_3 , $\text{NiCo}_2\text{O}_4/\text{WO}_3$ (NW), and $\text{NiCo}_2\text{O}_4/\text{WO}_3/\text{ACWH}$ (NWA) were synthesized simply through the hydrothermal method. The electrocatalytic behavior of these catalysts in the oxidation of methanol and ethanol was compared. The results show that the $\text{NiCo}_2\text{O}_4/\text{WO}_3/\text{ACWH}$ catalyst has a higher performance due to the synergistic effect of two metal oxides and the conductive role of ACWH. The $\text{NiCo}_2\text{O}_4/\text{WO}_3/\text{ACWH}$ catalyst with 98.6 and 95.7% current density stability in MOR and EOR processes after 2000 cyclic voltammetry cycles can be an attractive and stable option for use in alcohol fuel cell anodes.

2. Results and Discussion

2.1. Characterization of Catalysts

The crystal structure of the synthesized ACWH and NWA catalysts was studied by X-ray diffraction (XRD) analysis in the range of diffraction angles from 10 to 80 degrees. Figure 1 shows the XRD pattern of NWA and ACWH; the characteristic peaks shown at 16.3, 26.8, 33.0, 38.3, 47.4, 50.4, 55.3, 65.1, and 69.2 correspond to the Miller indices (111), (220), (222), (400), (422), (511), (440), (533), and (444), respectively. That is fully consistent with the JCPDS card number 01-073-1704 [50], which shows the presence of NiCo_2O_4 with a cubic structure and Fd-3m phase. Also, the diffraction angles of 18.4, 25.7, 31.5, 37.4, 49.6, 57.6, and 59.9 correspond to the Miller indices (−101), (011), (101), (−202), (−301), (−303), and (013) of WO_3 . These peaks correspond to the JCPDS card number 01-086-0134, which indicates the presence of WO_3 with a monoclinic structure and in the P21/n phase in the catalyst structure [51]. In the XRD pattern of ACWH, the characteristic peak of carbon is seen at the diffraction angle of about 27°.

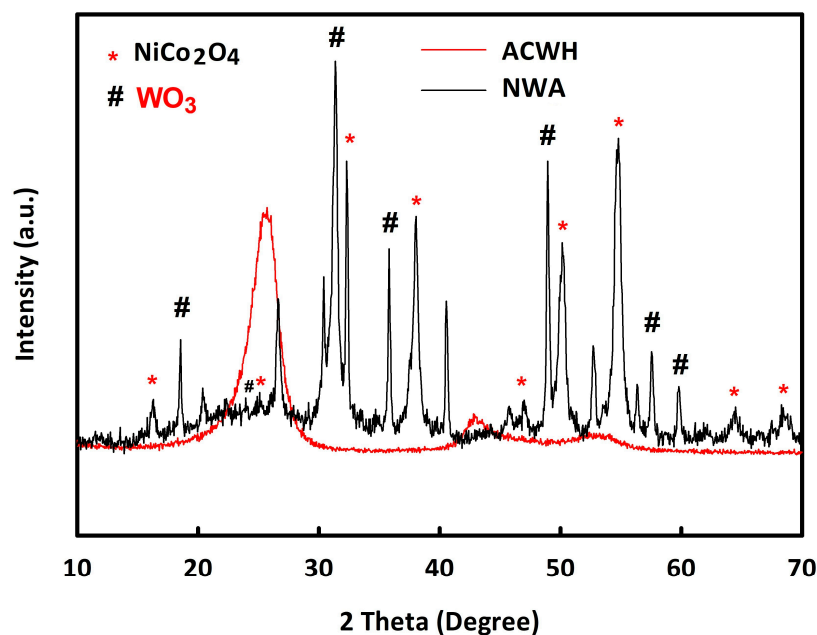


Figure 1. X-ray diffraction (XRD) patterns of NWA and ACWH.

The morphology of NWA and ACWH was investigated with FE-SEM analysis. As can be seen in Figure 2a–c, pores are observed on the surface of NiCo₂O₄/WO₃, and these pores can act as shortcuts for the passage and penetration of alcohol and electrolytes to the depth of the catalyst, which facilitates the oxidation process of alcohol. In addition, the porosities create more active sites for electrochemical reactions. Although the presence of ACWH as a substrate with an increasing active surface improves the electrocatalytic activity of the catalyst, the uniformity of the NiCo₂O₄/WO₃ catalyst on the surface of ACWH is also an important parameter for the greater efficiency of the catalyst. In Figure 2d, the structure of activated carbon obtained from wheat husk can be seen.

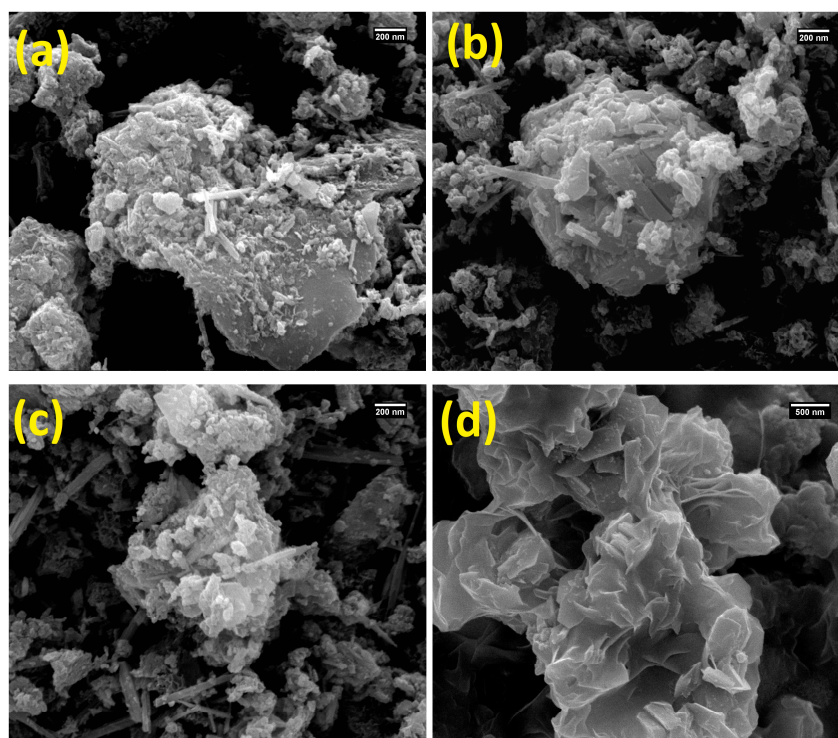


Figure 2. FE-SEM images of NWA (a–c) at the scale of 200 nm and ACWH at the scale of 500 nm (d).

2.2. Electrochemical Studies

2.2.1. Electrode Preparation

To modify the electrode, 50 mg of synthesized $\text{NiCo}_2\text{O}_4/\text{WO}_3$ and $\text{NiCo}_2\text{O}_4/\text{WO}_3/\text{ACWH}$ nanocatalysts was dispersed in 2 mL of ethanol and the 20 μL Nafion by sonication. A total of 4 μL of the obtained uniform slurry was placed on the surface of the glassy carbon electrode (GCE) and dried at 40 $^\circ\text{C}$ for 20 min. In the three-electrode system, the GCE modified with NW and NWA catalyst was used as the working electrode, and Ag/AgCl and platinum wire were used as the reference and auxiliary electrodes, respectively.

2.2.2. Investigation of MOR and EOR

The electrocatalytic activity of NW and NWA catalysts in methanol and ethanol oxidation was evaluated using electrochemical techniques in acidic and alkaline media. The CV diagrams of NW and NWA electrodes in 0.5 M KOH and 0.5 M H_2SO_4 solutions at the potential window of 0 to 1 V at the scan rate of 20 mV/s are shown in Figure 3a,b. From the figures, non-faradic and faradic current densities can be seen in both environments. The non-faradic current in an alkaline media is far more than the capacitive current in an acidic medium, which in a way expresses more and better activity of catalysts in an alkaline environment. Faradic current densities can be attributed to the redox reactions of NiCo_2O_4 and WO_3 .

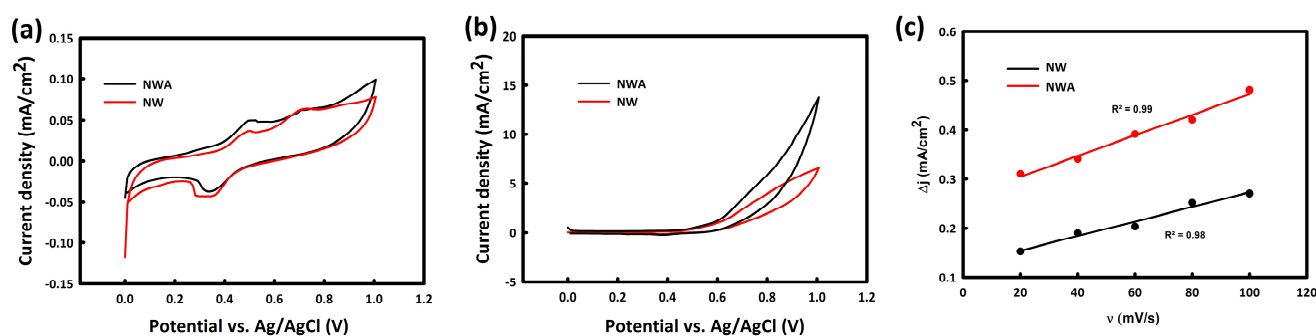


Figure 3. CV analysis of NW and NWA in acidic media (0.5 M H_2SO_4) (a) and alkaline media (0.5 M KOH) in the scan rate of 20 mV/s (b) and plots of Δj versus scan rate for NW and NWA (c) in 0.5 M KOH.

The electrochemical active surface area (ECSA) of a catalyst is directly related to the double-layer capacitance (C_{dl}) of the catalyst. So, C_{dl} values of catalysts were obtained from the capacitive current density of CV curves in different scan rates. By plotting Δj ($j_a = j_c$) at a potential of 0.25 V versus scan rate and linear fitting (Figure 3c), C_{dl} was obtained from half of the line slope. The C_{dl} values obtained were 1.05 and 0.75 mF/cm^2 for NW and NWA, respectively, indicating the higher activity of NWA due to the presence of ACWH in the matrix of the catalyst.

In the second step, to investigate the oxidation process of alcohols on the synthesized catalysts, CV analysis was performed in solutions containing 0.5 M KOH and 0.5 M H_2SO_4 electrolytes in the presence of 0.5 M methanol and 0.5 M ethanol.

Figure 4a,b show the behavior of NW and NWA in the presence of methanol and ethanol in an alkaline medium, respectively. As can be seen, in the presence of both alcohols, an oxidation peak is observed, which indicates the activity of both catalysts in the oxidation of methanol and ethanol in KOH media. NWA showed higher current density than NW due to the synergistic effect of metal oxides and ACWH and the conductive role of ACWH. Additionally, there are likely electronic interactions between $\text{NiCo}_2\text{O}_4/\text{WO}_3$ and ACWH. Electronic interactions have been reported in other similar works between rGO and $\text{NiCo}_2\text{O}_4/\text{MoS}_2$ [52] and silicon atoms with multi-walled carbon nanotubes [53].

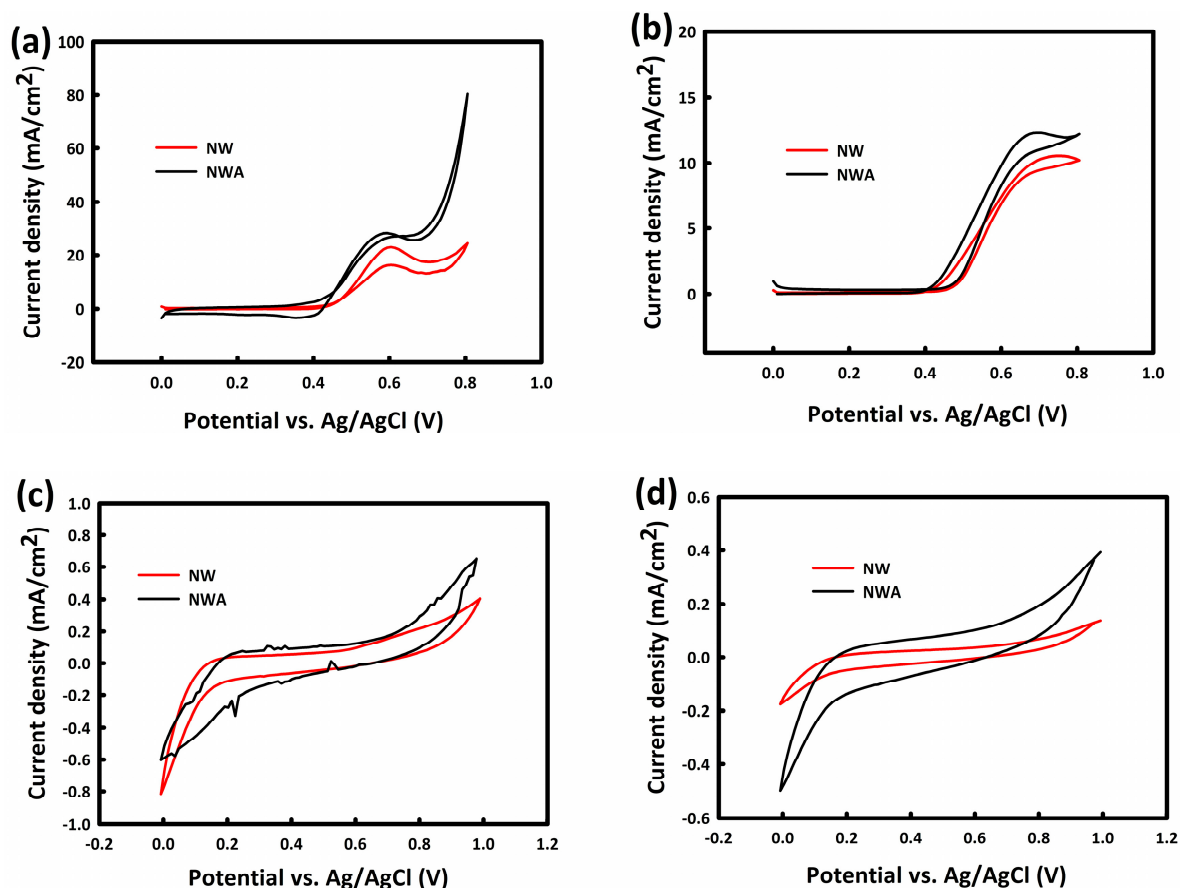


Figure 4. CV curves of NW and NWA in 0.5 M KOH/0.5 M methanol (a), 0.5 M KOH/0.5 M ethanol (b), 0.5 M H₂SO₄/0.5 M methanol (c), and 0.5 M H₂SO₄/0.5 M ethanol (d) at the scan rate of 20 mV/s.

Figure 4c,d also show the behavior of NW and NWA in an acidic environment, in the presence of 0.5 M methanol and ethanol, which indicates that no oxidation peak can be seen in the CV curves in acidic media. The proposed catalysts seem to have much better activity in the process of MOR and EOR in an alkaline environment.

According to the obtained results, the next electrochemical tests were investigated in an alkaline environment. The mechanism of alcohol oxidation on NW and NWA was investigated through CV analysis at different scan rates. Figure 5a,c show the CV curves of NW and NWA at the scan rates of 20 to 100 mV/s in 0.5 M KOH/0.5 M methanol and 0.5 M KOH/0.5 M ethanol, respectively. From Figure 5a,c, with increasing scan rate, an increase in the peak oxidation current density is seen. The plots of maximum current density in terms of the square root of the scan rate for NW and NWA catalysts (Figure 5b,d) indicate a linear relationship between these two parameters with $R^2 = 0.995$ and 0.993 , representing the diffusion control mechanism in the MOR process.

CV curves of NW and NWA in 0.5 M KOH/0.5 M ethanol at different scan rates are shown in Figure 6a,c, indicating current density increases similar to the MOR process. The linear relationship of maximum current density in terms of the square root of the scan rate for NW and NWA (Figure 6b,d) indicates the diffusion control mechanism in the EOR process, too.

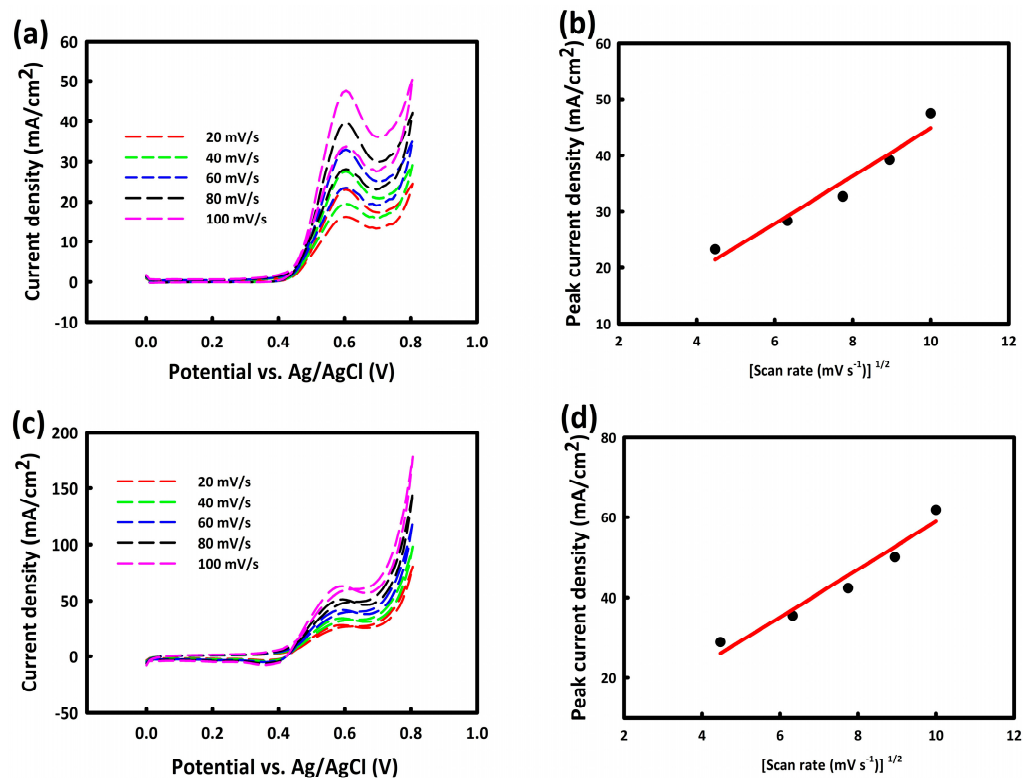


Figure 5. Cyclic voltammogram analysis of NW (a) and NWA (c) in 0.5 M KOH/0.5 M methanol at different scan rates. The maximum peak current density in terms of the square root of the scan rate for NW (b) and NWA (d).

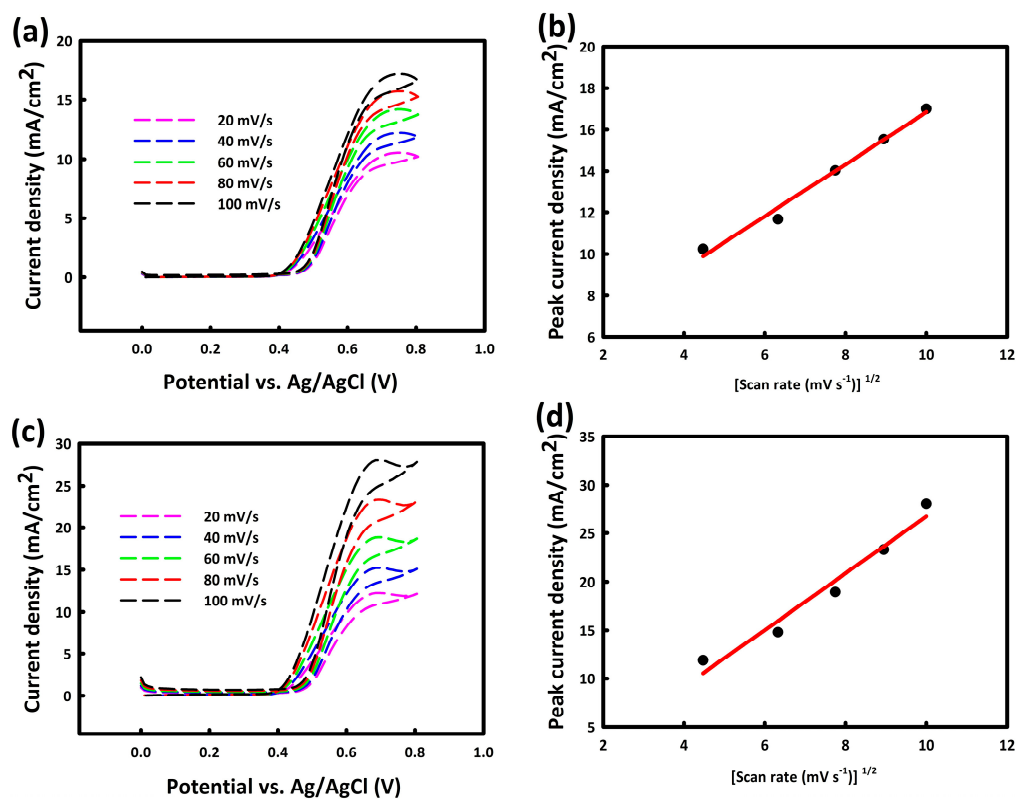


Figure 6. Cyclic voltammograms of NW (a) and NWA (c) in 0.5 M KOH/0.5 M ethanol at different scan rates. The maximum peak current density in terms of the square root of the scan rate for NW (b) and NWA (d).

To check the stability of NW and NWA catalysts in MOR and EOR processes, 2000 consecutive CV cycles at a scan rate of 100 mV/s in 0.5 M KOH/0.5 M methanol/ethanol were performed. As shown in Figure 7a,b, both nanocatalysts have excellent stability. The stability rate in the MOR process is 97.3% and 98.6% for NW and NWA, respectively. The stability of NW and NWA nanocatalysts in EOR was 93.5% and 95.7%, respectively (Figure 7c,d). The presence of ACWH increased the electrochemical active surface of the catalyst and improved the electrocatalytic activity of the $\text{NiCo}_2\text{O}_4/\text{WO}_3$ nanocatalyst.

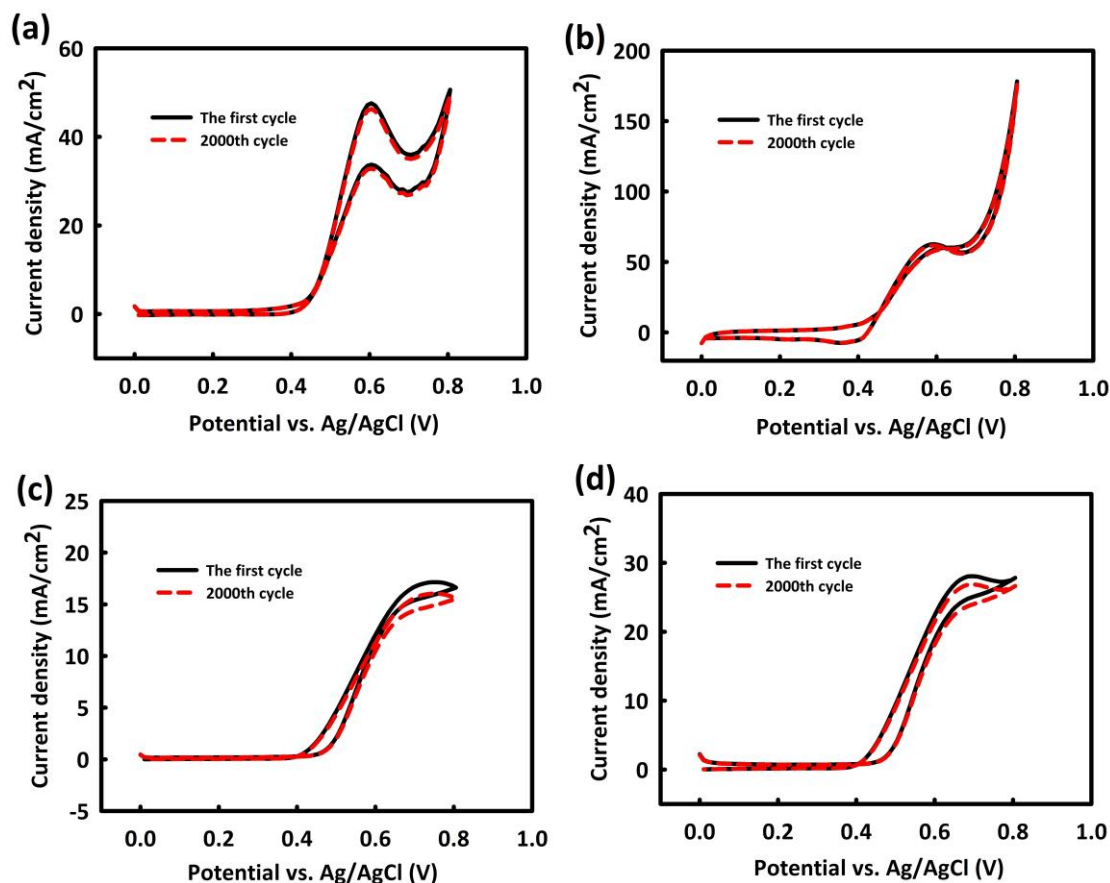


Figure 7. Cyclic stability of NW and NWA after 2000 consecutive CV cycles in MOR (a,b) and in EOR (c,d) at the scan rate of 100 mV/s in 0.5 M KOH/0.5 M methanol/ethanol.

The durability of the NWA catalyst for methanol and ethanol oxidation was evaluated by chronoamperometric measurements as shown in Figure 8. The remaining current densities after 3600 s were 92.8 and 85.7% for NWA in the presence of methanol and ethanol, respectively. According to the electrochemical results, the introduction of ACWH into the NW matrix increased the catalytic activity. The catalytic activity improvements of the NWA toward methanol oxidation were more significant than those on ethanol oxidation, indicating that NWA was a more efficient catalyst for methanol oxidation than ethanol oxidation.

Increasing the temperature facilitates the kinetics of oxidation and reduction reactions in fuel cells. To investigate the behavior of catalysts in MOR and EOR processes at different temperatures, CV analysis of catalysts was conducted at a scan rate of 100 mV/s in an ambient temperature range up to 50 °C. As is clear in Figure 9a,b, with increasing temperature, the oxidation current density increased for $\text{NiCo}_2\text{O}_4/\text{WO}_3$ and $\text{NiCo}_2\text{O}_4/\text{WO}_3/\text{ACWH}$ nanocatalysts in the MOR process. In the process of ethanol oxidation, it was also observed that with increasing temperature, the oxidation peak current density showed an increasing trend for two nanocatalysts (Figure 9c,d), or in other words, the oxidation process of methanol and ethanol is facilitated by increasing temperature.

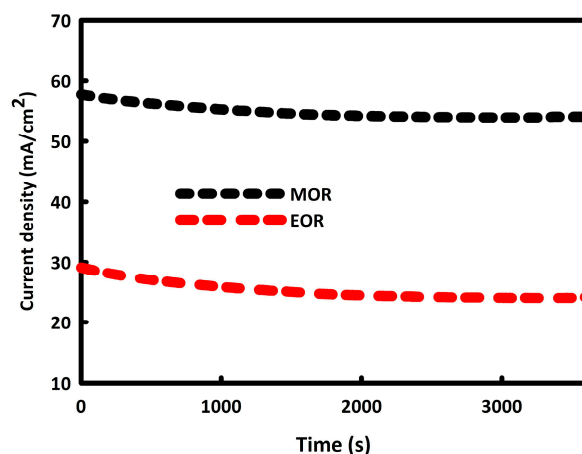


Figure 8. Chronoamperometry of NWA at the presence of 0.5 M methanol/0.5 M KOH and 0.5 M ethanol/0.5 M KOH at a constant potential of 0.6 V for 3600 s.

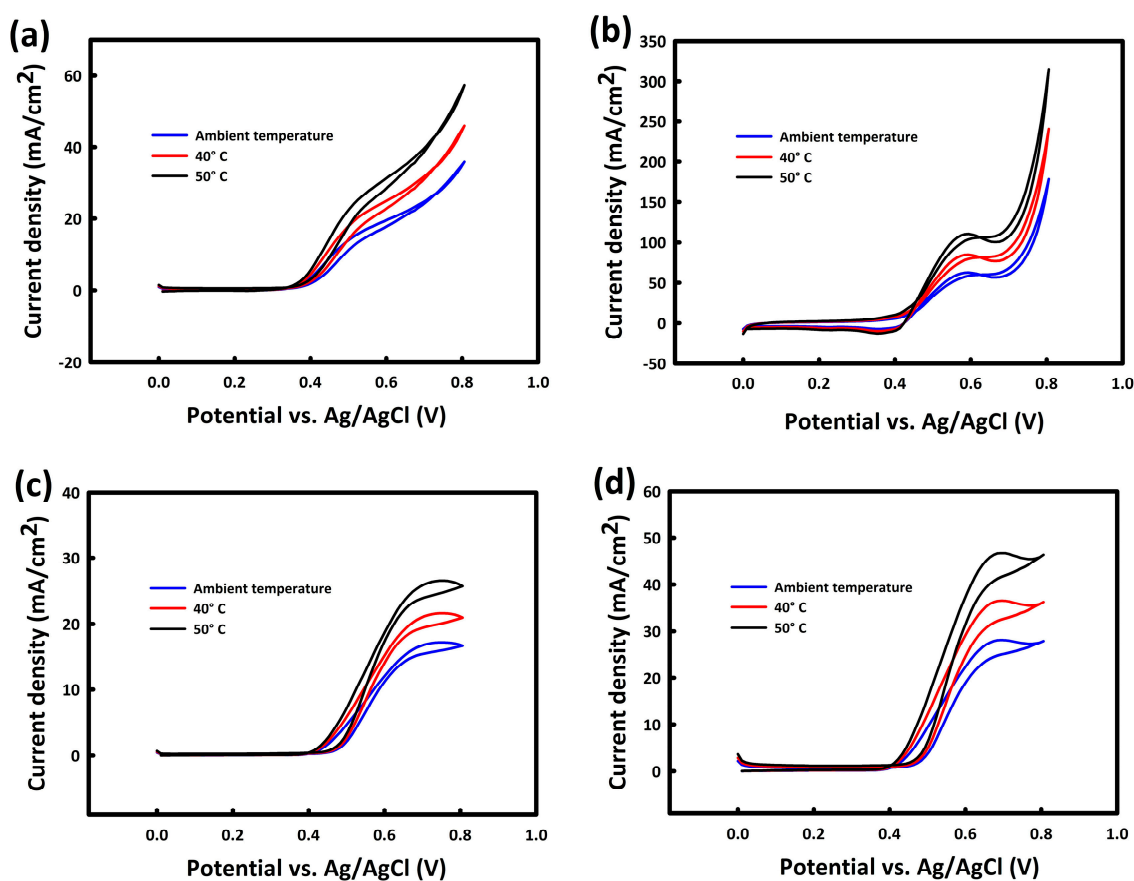


Figure 9. Cyclic voltammety of $\text{NiCo}_2\text{O}_4/\text{WO}_3$ and $\text{NiCo}_2\text{O}_4/\text{WO}_3/\text{ACWH}$ in MOR (a,b) and in EOR (c,d) at different temperatures.

The kinetics of electrode reactions on NW and NWA catalysts were investigated by electrochemical impedance spectroscopy at the frequency range of 100 kHz–0.1 Hz at the constant potential of 0.6 V. Nyquist plots of NW and NWA catalysts for methanol and ethanol electro-oxidation at a constant potential of 0.6 V are shown in Figure 10a,b. Both electrodes showed semi-circle plots. The ohmic resistance in the high-frequency region (the beginning of the semi-circle) corresponds to the solution resistance (R_s). The R_s values obtained were about 58 and 60 Ω in methanol (Figure 10a) and ethanol (Figure 10b) solutions, respectively.

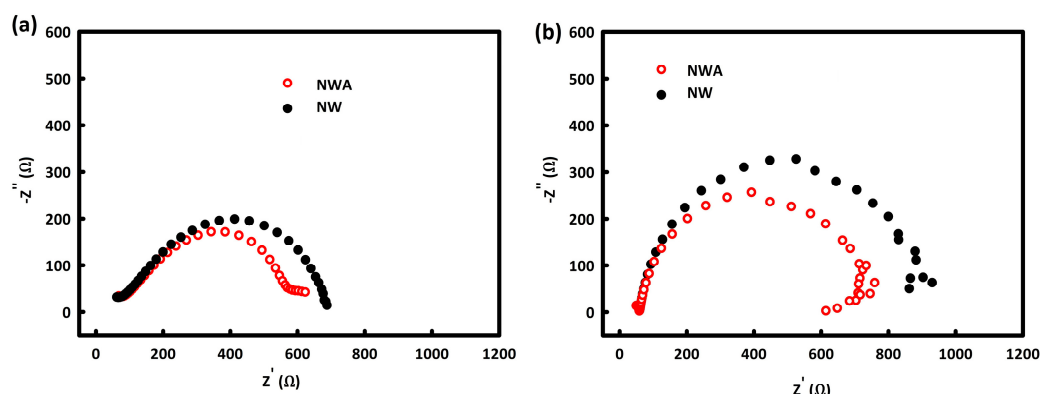


Figure 10. Nyquist plots of NW and NWA on MOR (a) and EOR (b) at the constant potential of 0.6 V in 0.5 M methanol and 0.5 M ethanol.

The diameter of the semi-circle is the charge transfer resistance (R_{ct}), representing the rate of charge transfer during methanol and ethanol electro-oxidation. The obtained values of R_{ct} for NW and NWA were 619 and 502 Ω in methanol oxidation and 843 and 730 Ω in ethanol oxidation, respectively. NWA shows lower R_{ct} , which indicates higher electrical conductivity of the electrode due to ACWH in the electrode matrix. Additionally, the methanol oxidation reaction rate is faster than the ethanol oxidation reaction on both catalysts.

The electrocatalytic activity of the NWA catalyst in the oxidation of methanol and ethanol in parameters such as oxidation current density, type and concentration of electrolyte and fuel, and oxidation peaks is compared with similar reported research in Table 1. The results show this catalyst is comparable with other similar reported catalysts in the literature. Although the electrocatalytic activity of the proposed catalysts is not comparable with platinum-based catalysts, NWA is a promising option for use in the anodes of alcohol fuel cells.

Table 1. Comparison of catalytic activity of NiCo₂O₄/WO₃/ACWH nanocatalyst in MOR and EOR with similar research.

| Electrocatalyst | Electrolyte Composition | Peak Potential (V) | Current Density (mA cm ⁻²) | Reference |
|---|--------------------------|----------------------------------|--|-----------|
| NWA | 0.5 M Methanol/0.5 M KOH | 0.58 vs. Ag/AgCl 1.59 vs. RHE | 63.39 | This work |
| NWA | 0.5 M Ethanol/0.5 M KOH | 0.67 vs. Ag/AgCl 1.68 vs. RHE | 27.98 | This work |
| ZnO(40%)/CeO ₂ (60%)dots@CNFs | 3 M Methanol/1 M KOH | 0.4 | 16.3 | [51] |
| NiCo ₂ O ₄ coral | 0.5 M Methanol/1 M KOH | 0.35 | 21 | [54] |
| ZrO ₂ /NiO/rGO | 0.5 M Ethanol/0.5 M KOH | 0.52 | 17.3 | [55] |
| Urchin-like NiCo ₂ O ₄ Hollow Microspheres | 0.5 M Methanol/1 M KOH | 1.6 | 33.8 | [56] |
| NiO/Ni-P Tube | 1 M Methanol/0.5 M KOH | 1.55 | 28.56 | [57] |
| NiO@PPC-600 | 1 M Ethanol/1 M KOH | 1.6 | 231.8 | [58] |
| np-CuO/TiO ₂ /Pd-NiO-3 | 0.5 M Ethanol/0.5 M NaOH | -0.3 | 2.614 | [59] |
| Pd-NiO/C | 3 M Ethanol/0.3 M KOH | -0.37 | 24.98 | [60] |
| NiCo ₂ O ₄ -rGO | 0.5 M Methanol/1 M KOH | 1.66 | 16.6 | [61] |
| MnCo ₂ O ₄ /NiCo ₂ O ₄ /rGO | 2 M Methanol/2 M KOH | 0.58 | 24.76 | [26] |

3. Experimental Section

3.1. Materials and Apparatus

The materials used were nitric acid (HNO₃), potassium hydroxide (KOH), sodium chloride (NaCl), sodium tungstate (Na₂WO₄), hydrochloric acid (HCl), methanol (CH₃OH), ethanol (C₂H₅OH), nickel nitrate (Ni(NO₃)₂), cobalt nitrate (Co(NO₃)₂), and urea (CH₄N₂O),

obtained from the Merck company (Rahway, NJ, USA). X-ray diffraction analysis was performed by a PW1730 (Philips, Tokyo, Japan). The surface morphology of nanocatalysts was investigated by an FE-SEM (VEGA3, TESCAN, Brno, Czech Republic). Electrochemical tests were performed on the Potentiostat/Galvanostat (Autolab PGSTAT302N, Metrohm, Herisau Switzerland) with a three-electrode system.

3.2. Synthesis of Catalysts

To carbonize wheat husk, 50 g of pure wheat husk was added to a 1 M nitric acid solution for 24 h in a stirrer at room temperature, and the resulting brown solution dried at 45 °C. The dried powder was poured into the NaOH solution to obtain a homogeneous slurry. After this step, the obtained product was placed in a vacuum oven at 400 °C for 3 h. The obtained product was combined with NaOH solution and dried at 100 °C.

For the synthesis of ACWH, 8 g of the carbonized wheat husk were dispersed in KOH solution (40 wt%) with a ratio of 1 to 4 by stirring and sonication, and then the resulting slurry was dried in the oven for 12 h at 60 °C. The product was annealed in an oven at 800 °C under argon gas. The obtained ACWH was washed with 0.1 M nitric acid solution until the pH of the solution reached 7 and finally dried at 40 °C.

For the synthesis of WO₃ by a simple hydrothermal method, NaCl was used as a capping agent, and sodium tungstate was used as a source of tungsten. In a typical synthesis, 3.2 g of Na₂WO₄·2H₂O and 1.1 g of NaCl were added to 60 mL of deionized water and stirred for 30 min. Next, 20 mL of 3 M HCl solution was added dropwise and slowly to the stirring solution, until the pH of the solution reached 2. Finally, the obtained solution was poured into an autoclave with a volume of 100 mL and placed in an oven at 180 °C for 24 h. After that, the product was washed with water/ethanol at a ratio of 1:1 with centrifugation and decantation five times and dried at 60 °C for 8 h.

For the synthesis of NiCo₂O₄/WO₃, the chemical precipitation method was used. For this purpose, 1 g of the obtained WO₃ powder was dispersed in 45 mL of deionized water by ultrasonication for 20 min and it was added to a solution containing 1 mmol of nickel nitrate, 2 mmol of cobalt nitrate, and 30 mmol of urea (CO(NH₂)₂). Next, the obtained product was stirred for 2 h at 75 °C. The obtained sediment was washed several times and dried at 70 °C for 6 h. Finally, the resulting powder was calcined at 350 °C for one hour.

To synthesize NiCo₂O₄/WO₃/ACWH, 0.5 g of the synthesized NiCo₂O₄/WO₃ was mixed with 0.04 g of ACWH into a beaker containing 40 mL of deionized water and sonicated for 1 h. The resulting mixture was transferred into a 50 mL autoclave and placed in the oven at 120 °C for 10 min. After the autoclave cooled down, the resulting material was washed several times with a mixture of deionized water and ethanol and dried at 70 °C. After calcining the resulting powder at 350 °C for one hour, the NiCo₂O₄/WO₃ / ACWH catalyst was obtained.

4. Conclusions

In this research, catalysts based on transition metal oxides were introduced as suitable inexpensive materials for application in the anode of alcohol fuel cells. A type of activated carbon derived from wheat husk was added to the matrix of the catalyst. ACWH increased the electrochemical active surface area of the catalyst, facilitated the oxidation process of alcohols, and improved the electrocatalytic activity of the catalyst. Both the NW and NWA catalysts indicated relatively good capabilities in MOR and EOR processes. NW and NWA showed a higher current density and a lower potential peak for MOR than EOR. The oxidation current density for NWA was 63.39 mA/cm² (at 0.58 V) in the MOR process and 27.98 mA/cm² (at 0.67 V) in EOR. The addition of ACWH increased the oxidation current density and enhanced the stability of the catalyst in chronoamperometric analysis by improving the electrochemical active surface area and electrical conductivity. The stability of NWA in the MOR and EOR processes was 98.6 and 95.7%, respectively, after 2000 CV cycles. In general, it can be said that both catalysts have good electrochemical

activity for the oxidation of alcohols and can be considered cheap and stable options in the anode structure of alcohol fuel cells.

Author Contributions: Conceptualization, M.B.A. and P.S.; methodology, M.B.A. and P.S.; software, M.B.A., S.R.S.H., M.S. and P.S.; validation, M.B.A. and S.A.; formal analysis, M.B.A., M.S. and P.S.; investigation, M.B.A. and P.S.; resources, M.B.A. and P.S.; data curation, M.B.A. and P.S.; writing—original draft preparation, M.B.A., M.S. and S.R.S.H.; writing—review and editing M.B.A. and P.S.; visualization, M.B.A. and S.A.; supervision, M.B.A.; project administration, M.B.A. All authors have read and agreed to the published version of the manuscript.

Funding: This research has been supported by the Institute of Science and High Technology and Environmental Sciences, Graduate University of Advanced Technology (Kerman-Iran) under grant number 02/1338.

Data Availability Statement: Data are available on request from the authors.

Conflicts of Interest: The authors declare no conflicts of interest.

References

- Sachs, J.D.; Woo, W.T.; Yoshino, N.; Taghizadeh-Hesary, F. Importance of green finance for achieving sustainable development goals and energy security. *Handb. Green Financ. Energy Secur. Sustain. Dev.* **2019**, *10*, 1–10.
- Kalair, A.; Abas, N.; Saleem, M.S.; Kalair, A.R.; Khan, N. Role of energy storage systems in energy transition from fossil fuels to renewables. *Energy Storage* **2021**, *3*, e135. [[CrossRef](#)]
- Fang, W.; Liu, Z.; Putra, A.R.S. Role of research and development in green economic growth through renewable energy development: Empirical evidence from South Asia. *Renew. Energy* **2022**, *194*, 1142–1152. [[CrossRef](#)]
- Halkos, G.E.; Gkampoura, E.-C. Reviewing usage, potentials, and limitations of renewable energy sources. *Energies* **2020**, *13*, 2906. [[CrossRef](#)]
- Cantarero, M.M.V. Of renewable energy, energy democracy, and sustainable development: A roadmap to accelerate the energy transition in developing countries. *Energy Res. Soc. Sci.* **2020**, *70*, 101716. [[CrossRef](#)]
- Chien, F.; Kamran, H.W.; Albashar, G.; Iqbal, W. Dynamic planning, conversion, and management strategy of different renewable energy sources: A sustainable solution for severe energy crises in emerging economies. *Int. J. Hydrogen Energy* **2021**, *46*, 7745–7758. [[CrossRef](#)]
- Bonenkamp, T.B.; Middelburg, L.M.; Hosli, M.O.; Wolffenbuttel, R.F. From bioethanol containing fuels towards a fuel economy that includes methanol derived from renewable sources and the impact on European Union decision-making on transition pathways. *Renew. Sustain. Energy Rev.* **2020**, *120*, 109667. [[CrossRef](#)]
- Li, Z.; Wang, Y.; Yin, Z.; Gao, Z.; Wang, Y.; Zhen, X. To achieve high methanol substitution ratio and clean combustion on a diesel/methanol dual fuel engine: A comparison of diesel methanol compound combustion (DMCC) and direct dual fuel stratification (DDFS) strategies. *Fuel* **2021**, *304*, 121466. [[CrossRef](#)]
- Dybiński, O.; Milewski, J.; Szabłowski, Ł.; Szcześniak, A.; Martinchuk, A. Methanol, ethanol, propanol, butanol and glycerol as hydrogen carriers for direct utilization in molten carbonate fuel cells. *Int. J. Hydrogen Energy* **2023**, *48*, 37637–37653. [[CrossRef](#)]
- Mohammed, H.; Al-Othman, A.; Nancarrow, P.; Tawalbeh, M.; Assad, M.E.H. Direct hydrocarbon fuel cells: A promising technology for improving energy efficiency. *Energy* **2019**, *172*, 207–219. [[CrossRef](#)]
- Rath, R.; Kumar, P.; Mohanty, S.; Nayak, S.K. Recent advances, unsolved deficiencies, and future perspectives of hydrogen fuel cells in transportation and portable sectors. *Int. J. Energy Res.* **2019**, *43*, 8931–8955. [[CrossRef](#)]
- Hassan, A.; Ilyas, S.Z.; Jalil, A.; Ullah, Z. Monetization of the environmental damage caused by fossil fuels. *Environ. Sci. Pollut. Res.* **2021**, *28*, 21204–21211. [[CrossRef](#)] [[PubMed](#)]
- He, Y.; Li, X.; Huang, P.; Wang, J. Exploring the road toward environmental sustainability: Natural resources, renewable energy consumption, economic growth, and greenhouse gas emissions. *Sustainability* **2022**, *14*, 1579. [[CrossRef](#)]
- Oskouei, M.Z.; Şeker, A.A.; Tunçel, S.; Demirbaş, E.; Gözel, T.; Hoccoğlu, M.H.; Abapour, M.; Mohammadi-Ivatloo, B. A critical review on the impacts of energy storage systems and demand-side management strategies in the economic operation of renewable-based distribution network. *Sustainability* **2022**, *14*, 2110. [[CrossRef](#)]
- Zhang, Z.; Ding, T.; Zhou, Q.; Sun, Y.; Qu, M.; Zeng, Z.; Ju, Y.; Li, L.; Wang, K.; Chi, F. A review of technologies and applications on versatile energy storage systems. *Renew. Sustain. Energy Rev.* **2021**, *148*, 111263. [[CrossRef](#)]
- Xu, H.; Shen, M. The control of lithium-ion batteries and supercapacitors in hybrid energy storage systems for electric vehicles: A review. *Int. J. Energy Res.* **2021**, *45*, 20524–20544. [[CrossRef](#)]
- Obileke, K.; Onyeaka, H.; Meyer, E.L.; Nwokolo, N. Microbial fuel cells, a renewable energy technology for bio-electricity generation: A mini-review. *Electrochem. Commun.* **2021**, *125*, 107003. [[CrossRef](#)]
- Fadzillah, D.M.; Kamarudin, S.K.; Zainoodin, M.A.; Masdar, M.S. Critical challenges in the system development of direct alcohol fuel cells as portable power supplies: An overview. *Int. J. Hydrogen Energy* **2019**, *44*, 3031–3054. [[CrossRef](#)]

19. Yun, Y. Alcohol fuels: Current status and future direction. In *Alcohol Fuels-Current Technologies and Future Prospect*; InTech Open: London, UK, 2020.
20. Hren, M.; Božič, M.; Fakin, D.; Kleinschek, K.S.; Gorgieva, S. Alkaline membrane fuel cells: Anion exchange membranes and fuels. *Sustain. Energy Fuels* **2021**, *5*, 604–637. [[CrossRef](#)]
21. Wang, P.; Cui, H.; Wang, C. Ultrathin PtMo-CeO_x hybrid nanowire assemblies as high-performance multifunctional catalysts for methanol oxidation, oxygen reduction and hydrogen oxidation. *Chem. Eng. J.* **2022**, *429*, 132435. [[CrossRef](#)]
22. Ren, X.; Wang, Y.; Liu, A.; Zhang, Z.; Lv, Q.; Liu, B. Current progress and performance improvement of Pt/C catalysts for fuel cells. *J. Mater. Chem. A* **2020**, *8*, 24284–24306. [[CrossRef](#)]
23. Alsolami, E.S.; Mkhaliid, I.A.; Shawky, A.; Hussein, M.A. Sol-gel assisted growth of nanostructured NiS/CeO₂ pn heterojunctions for fast photooxidation of ciprofloxacin antibiotic under visible light. *Appl. Nanosci.* **2023**, *13*, 6445–6455. [[CrossRef](#)]
24. Ma, X.; Liu, Y.; Wang, Y.; Jin, Z. Co₃O₄/CeO₂ pn heterojunction construction and application for efficient photocatalytic hydrogen evolution. *Int. J. Hydrogen Energy* **2021**, *46*, 33809–33822. [[CrossRef](#)]
25. Salarizadeh, P.; Askari, M.B.; Di Bartolomeo, A. MoS₂/Ni₃S₂/Reduced graphene oxide nanostructure as an electrocatalyst for alcohol fuel cells. *ACS Appl. Nano Mater.* **2022**, *5*, 3361–3373. [[CrossRef](#)]
26. Askari, M.B.; Azizi, S.; Moghadam, M.T.T.; Seifi, M.; Rozati, S.M.; Di Bartolomeo, A. MnCo₂O₄/NiCo₂O₄/rGO as a catalyst based on binary transition metal oxide for the methanol oxidation reaction. *Nanomaterials* **2022**, *12*, 4072. [[CrossRef](#)] [[PubMed](#)]
27. Narayanan, N.; Bernaurdshaw, N. Reduced graphene oxide supported NiCo₂O₄ nano-rods: An efficient, stable and cost-effective electrocatalyst for methanol oxidation reaction. *ChemCatChem* **2020**, *12*, 771–780. [[CrossRef](#)]
28. Gajraj, V.; Azmi, R.; Indris, S.; Mariappan, C.R. Boosting the Multifunctional Properties of MnCo₂O₄-MnCo₂S₄ Heterostructure for Portable All-Solid-State Symmetric Supercapacitor, Methanol Oxidation and Hydrogen Evolution Reaction. *ChemistrySelect* **2021**, *6*, 11466–11481. [[CrossRef](#)]
29. Sabzehmeidani, M.M.; Kazemzad, M.; Ebadzadeh, T. Bimetallic Au-Pd nanoparticles decorated electrospun spinel CoFe₂O₄ nanostructures as efficient electrocatalysts for ethanol fuel oxidation in alkaline media. *Int. J. Hydrogen Energy* **2023**, *51*, 517–528. [[CrossRef](#)]
30. Chen, L. β-Ni(OH)₂/NiFe₂O₄ heterostructure composite derived from layered double hydroxides precursor for ethanol oxidation electrocatalysis. *Int. J. Hydrogen Energy* **2023**, *48*, 26148–26161. [[CrossRef](#)]
31. Mary, B.C.J.; Vijaya, J.J.; Saravanakumar, B.; Bououdina, M.; Kennedy, L.J. NiFe₂O₄ and 2D-rGO decorated with NiFe₂O₄ nanoparticles as highly efficient electrodes for supercapacitors. *Synth. Met.* **2022**, *291*, 117201. [[CrossRef](#)]
32. Ye, J.; Cheng, B.; Yu, J.; Ho, W.; Wageh, S.; Al-Ghamdi, A.A. Hierarchical Co₃O₄-NiO hollow dodecahedron-supported Pt for room-temperature catalytic formaldehyde decomposition. *Chem. Eng. J.* **2022**, *430*, 132715. [[CrossRef](#)]
33. Noor, T.; Mohtashim, M.; Iqbal, N.; Naqvi, S.R.; Zaman, N.; Rasheed, L.; Yousuf, M. Graphene based FeO/NiO MOF composites for methanol oxidation reaction. *J. Electroanal. Chem.* **2021**, *890*, 115249. [[CrossRef](#)]
34. Zhao, J.; Zhang, Y.; Kang, X.; Li, Y. The preparation of NiO/Ni-N/C nanocomposites and its electrocatalytic performance for methanol oxidation reaction. *New J. Chem.* **2020**, *44*, 14970–14978. [[CrossRef](#)]
35. Askari, M.B.; Moghadam, M.T.T.; Azizi, S.; Hashemi, S.R.S.; Shojaeifar, M.; Di Bartolomeo, A. CeO₂-NiO-rGO as a nano-electrocatalyst for methanol electro-oxidation. *J. Phys. D Appl. Phys.* **2022**, *55*, 505501. [[CrossRef](#)]
36. Li, W.; Wen, X.; Wang, X.; Li, J.; Ren, E.; Shi, Z.; Liu, C.; Mo, D.; Mo, S. Oriented growth of δ-MnO₂ nanosheets over core-shell Mn₂O₃@δ-MnO₂ catalysts: An interface-engineered effects for enhanced low-temperature methanol oxidation. *Mol. Catal.* **2021**, *514*, 111847. [[CrossRef](#)]
37. Shi, Z.; Sun, G.; Yuan, R.; Chen, W.; Wang, Z.; Zhang, L.; Zhan, K.; Zhu, M.; Yang, J.; Zhao, B. Scalable fabrication of NiCo₂O₄/reduced graphene oxide composites by ultrasonic spray as binder-free electrodes for supercapacitors with ultralong lifetime. *J. Mater. Sci. Technol.* **2022**, *99*, 260–269. [[CrossRef](#)]
38. Yuan, R.; Chen, W.; Zhang, J.; Zhang, L.; Ren, H.; Miao, T.; Wang, Z.; Zhan, K.; Zhu, M.; Zhao, B. Crumpled graphene microspheres anchored on NiCo₂O₄ nanoparticles as an advanced composite electrode for asymmetric supercapacitors with ultralong cycling life. *Dalton Trans.* **2022**, *51*, 4491–4501. [[CrossRef](#)]
39. Prathap, M.A.; Srivastava, R. Synthesis of NiCo₂O₄ and its application in the electrocatalytic oxidation of methanol. *Nano Energy* **2013**, *2*, 1046–1053. [[CrossRef](#)]
40. Ko, T.H.; Devarayan, K.; Seo, M.K.; Kim, H.Y.; Kim, B.S. Facile synthesis of core/shell-like NiCo₂O₄-decorated MWCNTs and its excellent electrocatalytic activity for methanol oxidation. *Sci. Rep.* **2016**, *6*, 20313. [[CrossRef](#)]
41. Xu, H.; Zhao, L.; Liu, X.; Huang, Q.; Wang, Y.; Hou, C.; Hou, Y.; Wang, J.; Dang, F.; Zhang, J. Metal-organic-framework derived core-shell N-doped carbon nanocages embedded with cobalt nanoparticles as high-performance anode materials for lithium-ion batteries. *Adv. Funct. Mater.* **2020**, *30*, 2006188. [[CrossRef](#)]
42. Mersal, M.; Mohamed, G.G.; Zedan, A.F. Promoted visible-light-assisted oxidation of methanol over N-doped TiO₂/WO₃ nanostructures. *Opt. Mater.* **2021**, *122*, 111810. [[CrossRef](#)]
43. Asiri, A.M.; Nawaz, T.; Tahir, M.B.; Fatima, N.; Khan, S.B.; Alamry, K.A.; Alfifi, S.Y.; Marwani, H.M.; Al-Otaibi, M.M.; Chakraborty, S. Fabrication of WO₃ based nanocomposites for the excellent photocatalytic energy production under visible light irradiation. *Int. J. Hydrogen Energy* **2021**, *46*, 39058–39066. [[CrossRef](#)]
44. Khan, H.; Rigamonti, M.G.; Boffito, D.C. Enhanced photocatalytic activity of Pt-TiO₂/WO₃ hybrid material with energy storage ability. *Appl. Catal. B Environ.* **2019**, *252*, 77–85. [[CrossRef](#)]

45. Malode, S.J.; Prabhu, K.; Pollet, B.G.; Kalanur, S.S.; Shetti, N.P. Preparation and performance of WO_3/rGO modified carbon sensor for enhanced electrochemical detection of triclosan. *Electrochim. Acta* **2022**, *429*, 141010. [[CrossRef](#)]
46. Gopalakrishnan, A.; Badhulika, S. Hierarchical architected dahlia flower-like $\text{NiCo}_2\text{O}_4/\text{NiCoSe}_2$ as a bifunctional electrode for high-energy supercapacitor and methanol fuel cell application. *Energy Fuels* **2021**, *35*, 9646–9659. [[CrossRef](#)]
47. Kakarla, A.K.; Narsimulu, D.; Yu, J.S. Two-dimensional porous NiCo_2O_4 nanostructures for use as advanced high-performance anode material in lithium-ion batteries. *J. Alloys Compd.* **2021**, *886*, 161224. [[CrossRef](#)]
48. Li, Y.; Han, X.; Yi, T.; He, Y.; Li, X. Review and prospect of NiCo_2O_4 -based composite materials for supercapacitor electrodes. *J. Energy Chem.* **2019**, *31*, 54–78. [[CrossRef](#)]
49. Liu, T.; Zhang, X.; Fu, K.; Zhou, N.; Xiong, J.; Su, Z. Fabrication of $\text{Co}_3\text{O}_4/\text{NiCo}_2\text{O}_4$ nanocomposite for detection of H_2O_2 and dopamine. *Biosensors* **2021**, *11*, 452. [[CrossRef](#)]
50. Wang, P.; Wu, C.; Zhen, C.; Li, G.; Pan, C.; Ma, L.; Hou, D. Modulation of the structure and magnetic properties of the $\text{Ni}_{1-x}\text{Co}_2\text{-yO}_4$ powders by hydrothermal temperature. *Phys. B Condens. Matter* **2019**, *561*, 147–154. [[CrossRef](#)]
51. Abdullin, K.A.; Kalkozova, Z.K.; Markhabayeva, A.A.; Dupre, R.; Moniruddin, M.; Nuraje, N. Core-shell ($\text{W}@\text{WO}_3$) nanostructure to improve electrochemical performance. *ACS Appl. Energy Mater.* **2018**, *2*, 797–803. [[CrossRef](#)]
52. Ran, J.; Liu, Y.; Feng, H.; Zhan, H.; Yang, S. Rapid hydrothermal green synthesis of core-shell-shaped $\text{NiCo}_2\text{O}_4@\text{MoS}_2/\text{RGO}$ ternary composites for high-performance electrode materials. *J. Ind. Eng. Chem.* **2023**, *133*, 273–283. [[CrossRef](#)]
53. Oke, J.A.; Idisi, D.O.; Sarma, S.; Moloi, S.J.; Ray, S.C.; Chen, K.H.; Ghosh, A.; Shelke, A.; Pong, W.F. Electronic, electrical, and magnetic behavioral change of SiO_2 -NP-decorated MWCNTs. *ACS Omega* **2019**, *4*, 14589–14598. [[CrossRef](#)]
54. Yu, M.; Wang, S.; Hu, J.; Chen, Z.; Bai, Y.; Wu, L.; Chen, J.; Weng, X. Additive-free macroscopic-scale synthesis of coral-like nickel cobalt oxides with hierarchical pores and their electrocatalytic properties for methanol oxidation. *Electrochim. Acta* **2014**, *145*, 300–306. [[CrossRef](#)]
55. Askari, M.B.; Beitollahi, H.; Di Bartolomeo, A. Methanol and Ethanol Electrooxidation on $\text{ZrO}_2/\text{NiO}/\text{rGO}$. *Nanomaterials* **2023**, *13*, 679. [[CrossRef](#)]
56. Yu, X.Y.; Yao, X.Z.; Luo, T.; Jia, Y.; Liu, J.H.; Huang, X.J. Facile synthesis of urchin-like NiCo_2O_4 hollow microspheres with enhanced electrochemical properties in energy and environmentally related applications. *ACS Appl. Mater. Interfaces* **2014**, *6*, 3689–3695. [[CrossRef](#)]
57. Tong, Y.Y.; Gu, C.D.; Zhang, J.L.; Tang, H.; Wang, X.L.; Tu, J.P. Thermal growth of NiO on interconnected Ni–P tube network for electrochemical oxidation of methanol in alkaline medium. *Int. J. Hydrogen Energy* **2016**, *41*, 6342–6352. [[CrossRef](#)]
58. Gao, N.; Gao, L.; Zhang, X.; Zhang, Y.; Hu, T. NiO nanocrystal anchored on pitaya peel-derived carbon laminated mesoporous composites for the electrocatalytic oxidation of ethanol. *J. Alloys Compd.* **2023**, *947*, 169485. [[CrossRef](#)]
59. Niu, M.; Xu, W.; Zhu, S.; Liang, Y.; Cui, Z.; Yang, X.; Inoue, A. Synthesis of nanoporous $\text{CuO}/\text{TiO}_2/\text{Pd-NiO}$ composite catalysts by chemical dealloying and their performance for methanol and ethanol electro-oxidation. *J. Power Sources* **2017**, *362*, 10–19. [[CrossRef](#)]
60. López-Rico, C.A.; Galindo-De-La-Rosa, J.; Ortiz-Ortega, E.; Álvarez-Contreras, L.; Ledesma-García, J.; Guerra-Balcázar, M.; Arriaga, L.G.; Arjona, N. High performance of ethanol co-laminar flow fuel cells based on acrylic, paper and Pd-NiO as anodic catalyst. *Electrochim. Acta* **2016**, *207*, 164–176. [[CrossRef](#)]
61. Umeshbabu, E.; Rao, G.R. NiCo_2O_4 hexagonal nanoplates anchored on reduced graphene oxide sheets with enhanced electrocatalytic activity and stability for methanol and water oxidation. *Electrochim. Acta* **2016**, *213*, 717–729. [[CrossRef](#)]

Disclaimer/Publisher’s Note: The statements, opinions and data contained in all publications are solely those of the individual author(s) and contributor(s) and not of MDPI and/or the editor(s). MDPI and/or the editor(s) disclaim responsibility for any injury to people or property resulting from any ideas, methods, instructions or products referred to in the content.